ULTRASONIC REFLECTION AND WAVE PROPAGATION IN MULTILAYERED COMPOSITE PLATES

D. E. Chimenti
Materials Laboratory
Wright-Patterson Air Force Base, OH 45433

Adnan H. Nayfeh
Aerospace Engineering and Engineering Mechanics
University of Cincinnati
Cincinnati, OH 45221

INTRODUCTION

This paper presents selected results of numerous ultrasonic reflection measurements on plates of laminated composites in which the angle of incidence of the acoustic wave and its frequency have been varied. These measurements have been carried out on biaxially laminated graphite-epoxy specimens utilizing water as a fluid coupling medium. The stacking sequence of the samples investigated is restricted to the case of 0-90° lamination. The data are compared to the results of a recent theoretical analysis based on an exact analytical treatment of wave propagation in a fluid-coupled orthotropic plate in conjunction with a transfer matrix approach. Reflection and transmission coefficients are derived for the multilayer anisotropic laminate from which the characteristic behavior of the system is identified. In general, very good agreement is found between prediction and experiment. Moreover, significant changes in the reflection spectra are observed and predicted, depending on the orientation of the composite plates.

In several recent papers [1-3] we have examined analytically and experimentally the interaction of ultrasonic waves with unidirectional fibrous composite plates immersed in water. With the plate wavevector oriented parallel to the fiber direction, dispersion-like curves of phase velocity versus normalized plate thickness have been constructed from reflection data for a graphite-epoxy plate, demonstrating anomalous behavior in the lowest order symmetric mode [1]. A more detailed treatment of the character and possible source of the anomaly, along with the derivation of an analytical expression for the reflection coefficient of a transversely isotropic plate, has also appeared [2]. More recently [3], these results have been extended to include the case of plate wave propagation at arbitrary angles to the fiber direction, clearly showing the influence of coupling to SH-like particle motion. In addition, since these last two contributions contain extensive reviews of the relevant literature in this area, we will not repeat that background here.

THEORETICAL SUMMARY

The analysis of this problem proceeds from our earlier calculation on a single-layer fluid-coupled plate, which can have orthotropic or higher symmetry. Referring to the geometry of Fig. 1, we introduce a local coordinate system $x_{i(k)}$ with its origin at the interface of the k and k-1 layers. Hence, layer k occupies the space $0 \le x_{3(k)} \le d_k$, where d_k is the thickness of that layer. To simplify the exposition we further assume that guided wave propagation in the multilayered structure is always along one of the two in-plane principal material axes. In that case there will be no x_2 particle motion, and all field variables will be independent of x_2. At the plate-fluid interface the normal stress and displacement are conserved across the boundary and the shear stress vanishes. At the lamina interfaces, however, normal and in-plane displacements and normal and shear stresses are continuous, as usual.

For each layer the equations of motion are combined into simultaneous equations for the displacements u_1 and u_3, and we postulate the formal solution

$$(u_1, u_2) = (U, W) \exp\left(i\, q\, (x_1 + \alpha x_3)\right) \tag{1}$$

where U and W are displacement amplitudes, q is the x_1 wavenumber, and α is the ratio of the x_3 and x_1 wavenumbers. Requiring nontrivial solutions to the resulting equations, one obtains a characteristic equation for α. This equation admits four solutions, extensional and transverse waves propagating with positive and negative x_3 wavevector components. By superposition we finally have

$$(u_1,\, u_3,\, \sigma_{33},\, \sigma_{13})_k =$$

$$\sum_{m=1}^{4} (1,\, W_m,\, D_{1m},\, D_{2m})_k\, U_m \exp(i\, q\, (x_1 + \alpha_m x_3)) \tag{2}$$

where the α_m, W, D_1, D_2 are given in ref. [3]. Equation (2) can now be used to relate stresses and displacements at $x_{3(k)} = 0$ to those at $x_{3(k)} = d_k$. Substituting 0_k and d_k into Eq.(2), and eliminating the common amplitude column of U_m yields

$$F_i\,(d_k) = [a_{ij}]_k\, F_j\,(0_k), \tag{3}$$

where F_i designates the field variables $u_1, u_3, \sigma_{33}, \sigma_{13}$, respectively. The $[a_{ij}]$ are matrices composed of the anisotropic elastic properties of each layer and given in ref. [4].

Continuing this procedure for each layer and satisfying the continuity conditions at the interfaces leads to relations between field variables at the top and bottom surfaces of the plate. Using the transfer-matrix approach [5] we have

$$F_i\,(d) = [A_{ij}]\, F_j\,(0), \tag{4}$$

where $[A_{ij}] = [a_{ij}]_n\, [a_{ij}]_{n-1} \ldots [a_{ij}]_1$. Combining this result with the solutions of the equations of motion in the fluid and subjecting these to the boundary conditions yields the reflec-

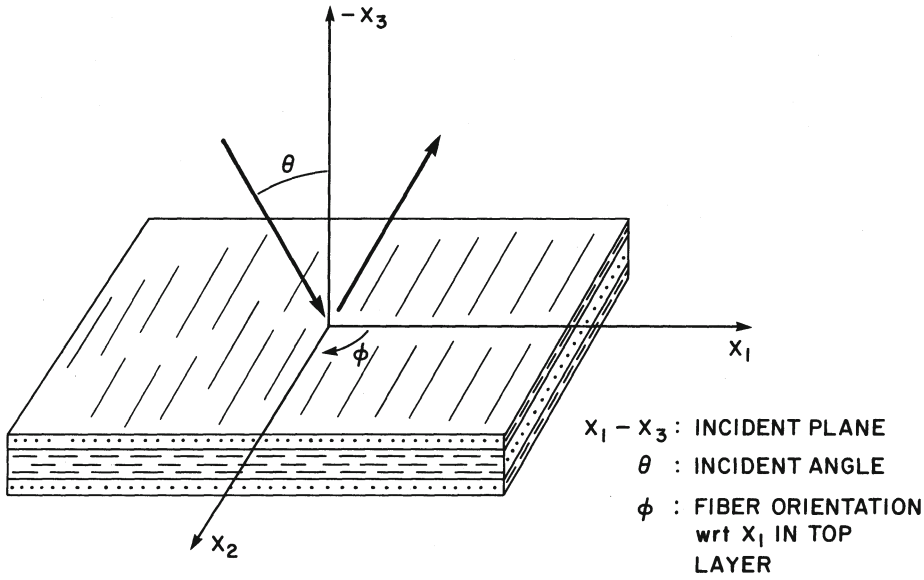

Fig. 1. Experimental geometry of biaxially laminated composite plates. Vectors at origin denote incident and reflected waves. ϕ is angle of fibers in uppermost ply with respect to the incident plane.

tion coefficient for the fluid-coupled multilayered plate of orthotropic laminae,

$$R = \frac{[M_{21} + QM_{22} - Q(M_{11} + QM_{12})]}{[M_{21} + QM_{22} + Q(M_{11} + QM_{12})]} \tag{5}$$

where $Q=\rho_f c^2/\alpha_f$ c is the guided wavespeed, and α_f is the x_3 wavenumber in the fluid. The terms M_{ij} are related, through the $[A_{ij}]$, to the elastic constants of the materials comprising the layers and are given explicitly in ref. [4].

EXPERIMENTAL TECHNIQUE

The analysis of wave propagation in terms of reflection properties of the fluid-coupled structure under study is a well established approach [6]. It has been used by us in our previous work on both Rayleigh and Lamb waves. To obtain the reflection characteristics of fluid-coupled plates we direct a sound beam from an ultrasonic piston transducer onto the surface of the plate at a chosen angle. The plate normal vector and the incident sound wavevector define the incident plane of the ultrasound. A second transducer of nominally identical frequency bandwidth and sensitivity characteristics, whose axis is also in the incident plane, receives the reflected signal from the plate. The receiver is oriented at the negative incident angle, and the point of intersection of its axis with the surface of the plate may either coincide with that of the incident transducer or may be displaced from it in the propagation direction. Detailed descriptions of the experimental geometry and the excitation waveforms for these measurements have been presented elsewhere [3,7] and will not be repeated here.

In these experiments we have investigated two samples of graphite-epoxy composite, both biaxial laminates. These composites have been fabricated from Hercules AS/4 fibers and 3501 epoxy. Fiber volume fraction is measured to be 0.67. We have

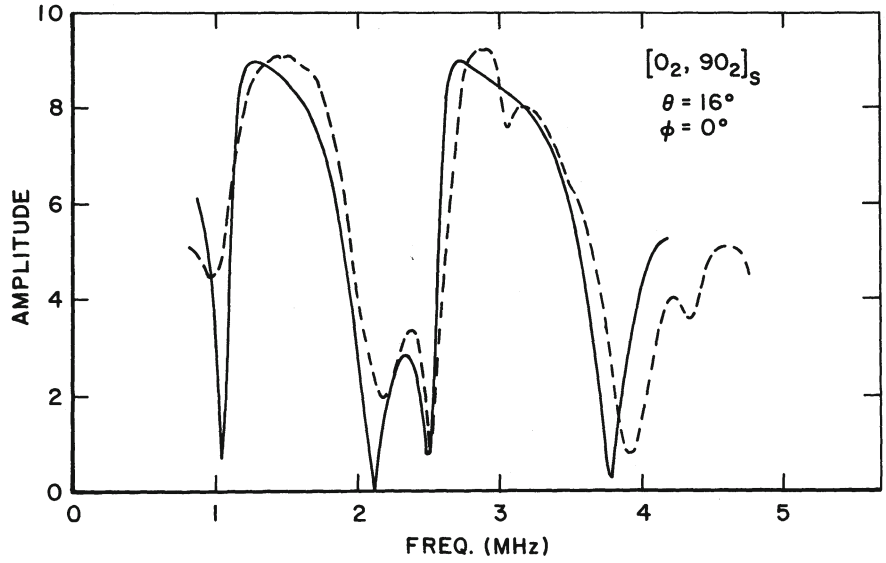

Fig 2. Reflection spectrum for $[0_2, 90_2]_s$ laminate. Experiment is dashed curve, while theory is solid curve.

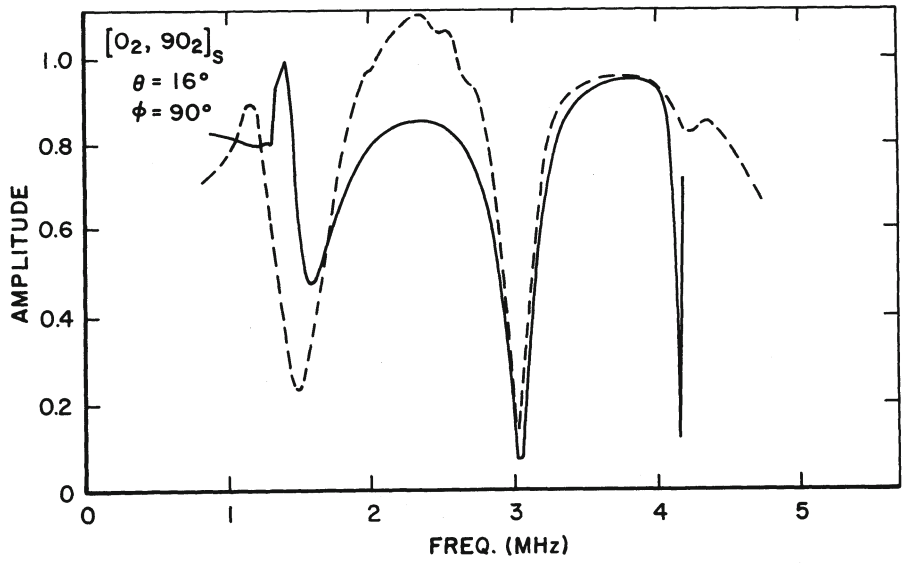

Fig 3. As in Fig. 2, but with $\phi = 90^{\circ}$.

taken literature values [8] for the elastic constants. The biaxial samples are $[0_2, 90_2]_s$ with 8 plies and $[0,90]_{3s}$ having 12 plies. Sample thicknesses are 1.00 and 1.52 mm, respectively, where we have estimated the sonic thickness from the physical thickness by subtracting 0.02 mm for the impressions left by the bleeder cloths. No special treatment was applied to the specimens. As a result, some variation in elastic behavior and thickness could be observed in ultrasonic survey scans across these samples. The data we present require very little manipulation for direct comparison to the model calculations. Normalization of the frequency spectra removes the transducer response function from the data. This step is performed by dividing the interpolated video-detected halfspace reflection spectrum into the experimental video signal.

The experimental use of finite-aperture piston transducers implies that an additional analysis procedure should be performed to compare the measured spectra with the calculations, which yield the plane-wave reflection coefficient. A finite ultrasonic beam is composed of an angular spectrum of plane wave components which define its profile. After its interaction with the plate, each component of the incident beam will contribute to the reflected field weighted by the appropriate value of the reflection coefficient for that incident angle θ. Therefore, the reflected field can be represented by the sum of these contributions,

$$A(x_i, fd) = \int_{-\infty}^{\infty} R(\xi, fd)\, \hat{\beta}(\xi) \exp i\,\xi(x_1 + \alpha x_3)\, d\xi \qquad (6)$$

where $R(\xi, fd)$ is the reflection coefficient from Eq. (5) for the composite plate and $\beta(\xi)$ is the incident beam spectrum. The expression of Eq. (6) evaluated over frequency is a one-dimensional approximation to the reflection spectrum of the plate, where the beam profile $\beta(x)$ is chosen to approximate the incident beam.

RESULTS AND DISCUSSION

For the case of the biaxially laminated composites dispersion curves are of less interest, since the behavior in these samples is clearly structure-dependent. We have represented the results instead as frequency spectra from which dispersion curves could be developed. An example of experimental and theoretical curves for a four-layer biaxial composite $[0_2, 90_2]_s$ is shown in Fig. 2. The dashed curve is the measurement, while the calculation is demonstrated as a solid curve. Only the relative amplitudes of the two curves have been scaled, since absolute reflectance has not been measured. An incident angle of 16° is selected, and the fiber direction in the upper layer is in the incident plane. Although the finite beam calculation outlined above has not been performed on the plane-wave reflection coefficient, comparison with the experimental data is still very good; nearly all details of the data are reproduced in the calculation. Since most of the data has been collected with no displacement between the two transducer sensitivity axes, little change other than a decrease in the sharpness of the minima should be seen in the theory curve after a recalculation according to Eq. (6).

Figure 3 shows the result of rotating the incident plane by 90° while maintaining a 16° incident angle, so that the upper fiber layer is perpendicular to the wave propagation direction. The experimental reflection spectrum is markedly different, both in appearance and precise location of the minima. Yet the model calculation follows the data very well. This case, and many others we have examined, exemplify the complex nature

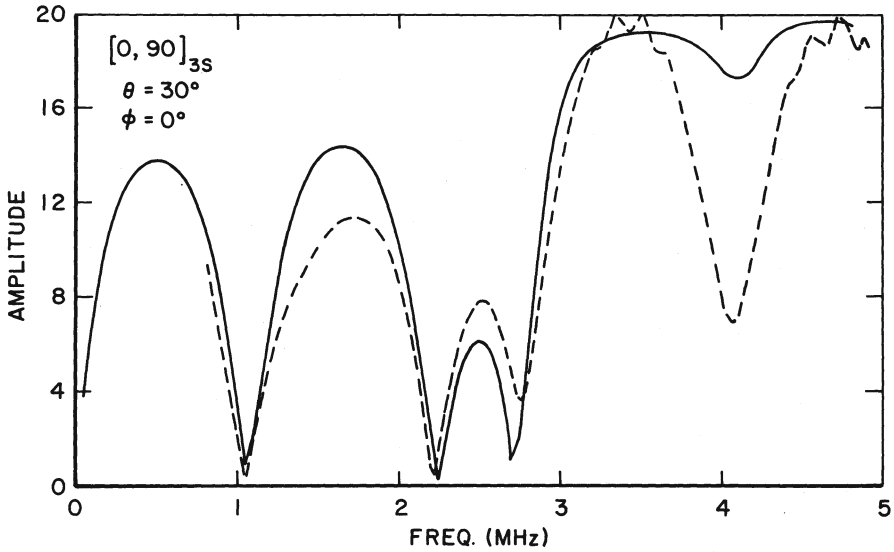

Fig. 4. Reflection spectrum for $[0,90]_{3s}$ laminate at incident angle of 30°. Experimental curve is dashed, theory is solid.

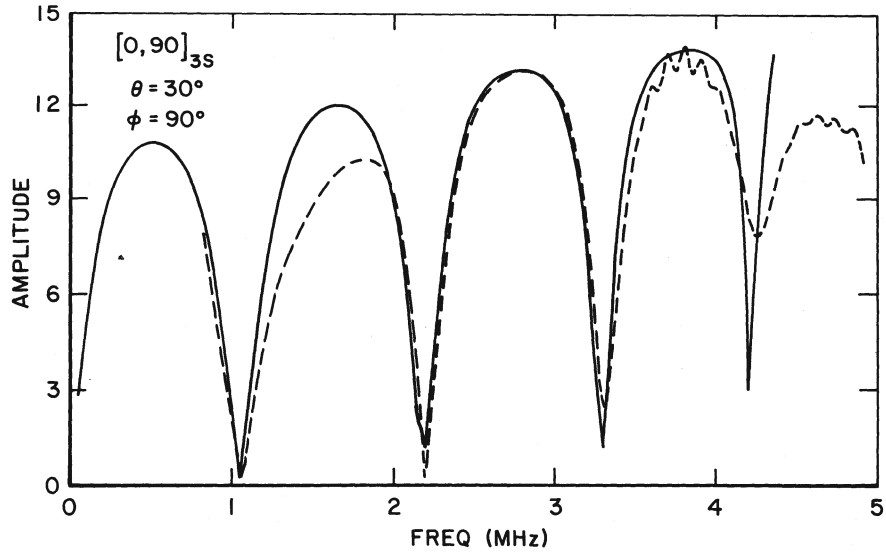

Fig. 5. As in Fig. 4, but with ϕ =90°.

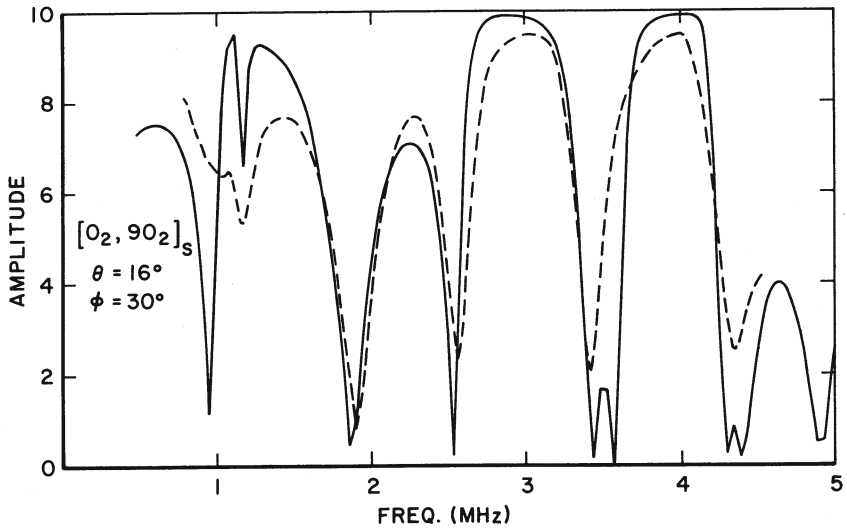

Fig. 6. Reflection spectrum for $[0_2, 90_2]_s$ laminate with $\theta = 16^\circ$ and $\phi = 30^\circ$. Dashed curve is experiment, solid curve is theory.

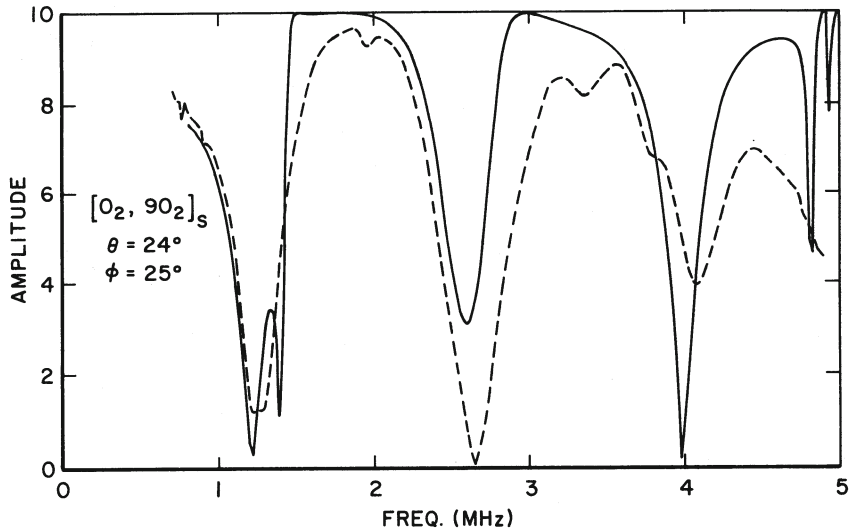

Fig. 7. As in Fig. 6 with $\theta = 24^\circ$ and $\phi = 25^\circ$.

of ultrasonic reflection in layered orthotropic materials. Clearly, a simpler model consisting only of mechanical properties averaged through the plate thickness would be unable to account for the difference between the data in Figs. 2 and 3.

A much more complicated situation is presented by a 12-ply laminate having an alternating structure in each layer. The lay-up scheme for this sample is $[0,90]_{3S}$. Figure 4 shows measurements for an incident angle of 30° and the upper layer fibers in the incident plane. In Fig. 5 the incident plane is rotated 90°. Comparison of these two cases reveals that even with as many as 12 alternating layers, the order of the anisotropic layers is still important. The minima near 1 and 2 MHz are basically constant between the two cases, but significant differences in the structure of the curve minima occur above this frequency. These variations can be attributed only to the order of layering, a relatively surprising result since only the slow transverse quarter wavelength in the 90° layers is approaching the layer thickness.

If we now rotate the sample through an angle other than 90°, neither principal axis will lie in the incident plane. This situation corresponds to the most general orthotropic multilayered problem, equivalent to a quasi-isotropic laminate. The analysis requires a moderate increase in complexity over the summary given above [4]. Figures 6 and 7 show the reflection spectra from the $[0_2, 90_2]_S$ plate at incident and rotation angles of 16° and 30°, and 24° and 25°, respectively. Since no special care has been taken in the preparation of the composite samples, nonuniformities in ply thickness or fiber orientation and density could account for the modest differences between prediction and experiment. In spite of these minor disparities, most features in the experimental spectra are reproduced in the calculation.

REFERENCES

1. D. E. Chimenti and A. H. Nayfeh, Appl. Phys. Lett. 49, 492 (1986).
2. A. H. Nayfeh and D. E. Chimenti, J. Acoust. Soc. Am. 83, 1736 (1988).
3. A. H. Nayfeh and D. E. Chimenti, J. Appl. Mech., to appear Dec (1988).
4. A. H. Nayfeh, T. W. Taylor, and D. E. Chimenti, in Wave Propagation in Structural Composites, edited by A. K. Mal and T. C. T. Ting (ASME, New York, 1988), AMD-Vol. 90, p.17.
5. L. M. Brekhovskikh, Waves in Layered Media, (Academic Press, New York, 1980), Chap. 1.
6. A. Schoch, Acustica 2, 1 (1952).
7. D. E. Chimenti and A. H. Nayfeh, in Wave Propagation in Structural Composites, *op. cit.*, p. 29.
8. R. D. Kriz and W. W. Stinchcomb, Exp. Mech. 19, 41 (1979).